Avalanche dynamics, surface roughening, and self-organized criticality: Experiments on a three-dimensional pile of rice

C. M. Aegerter, R. Günther, and R. J. Wijngaarden
Division of Physics and Astronomy, Faculty of Sciences, Vrije Universiteit, De Boelelaan 1081, 1081HV Amsterdam, The Netherlands
(Received 28 November 2002; published 27 May 2003)

We present a two-dimensional system that exhibits features of self-organized criticality. The avalanches that occur on the surface of a pile of rice are found to exhibit finite size scaling in their probability distribution. The critical exponents are $\tau=1.21(2)$ for the avalanche size distribution and $D=1.99(2)$ for the cutoff size. Furthermore, the geometry of the avalanches is studied, leading to a fractal dimension of the active sites of $d_B=1.58(2)$. Using a set of scaling relations, we can calculate the roughness exponent $\alpha=D-d_B=0.41(3)$ and the dynamic exponent $z=D(2-\tau)=1.56(8)$. This result is compared with that obtained from a power-spectrum analysis of the surface roughness, which yields $\alpha=0.42(3)$ and $z=1.5(1)$ in excellent agreement with those obtained from the scaling relations.

DOI: 10.1103/PhysRevE.67.051306 PACS number(s): 45.70.Ht, 05.65.+b, 89.75.−k

I. INTRODUCTION

The concept of self-organized criticality (SOC) [1] presents a simple way of modeling slowly driven, out of equilibrium systems. The interesting natural systems thought to exhibit SOC, such as rainfall [2], earthquakes [3], economic markets [4], biological evolution [5], or the brain [6], are difficult to study in a controlled experiment, and more simple systems have to be found with which the predictions of SOC can be tested quantitatively. Among the first toy systems studied were sand piles; however, it has been shown that due to the appearance of, e.g., kinetic effects, real sand does not behave like an SOC system [7]. Another system that has shown indications of SOC in a controlled environment is the dynamics of vortices in type-II superconductors. Here, power-law scaling has been observed in the past [8], however, not all authors have found avalanche scaling [9]. This is probably due to the fact that internal avalanches are not measured in the usual setup [10]. Recently, Behnia *et al.* [11] have measured internal avalanches using arrays of Hall probes, where they do indeed find a power-law behavior of the avalanches. The ultimate hallmark of SOC, however, is the observation of finite size scaling, indicating a true critical dynamics. So far, there are only two experimental systems, a one-dimensional (1D) pile of rice [12] or a 1D pile of steel balls with a random arrangement at its bottom layer [13], which have been shown to exhibit finite size scaling in their avalanche distributions.

The critical exponents obtained from a finite size scaling analysis would yield more information on an SOC system, as was discussed by Paczuski *et al.* [14] for models in a stationary critical state. A system evolving through avalanches, which are distributed according to a power law, will also show roughening dynamics of its surface. This can be seen as an indication to the origin of the abundance of fractal or self-affine structures in nature. Roughening dynamics has been studied extensively in the past, including the study of interfaces in porous media [15], the growth of bacterial colonies [16], the slow combustion [17], or the rupture [18] of paper. These systems are well characterized experimentally and in many cases, the interface dynamics can be modeled analytically by the Kardar-Parisi-Zhang (KPZ) equation [19]. In one spatial dimension, the KPZ equation is solved exactly for the case of white noise, such that a good comparison between experiment and theory is possible. However, e.g., in the burning of paper, there are avalanches observed in the propagation of the front, which are reminiscent of SOC dynamics [20]. This has recently been addressed by Alava and co-workers [21], who proposed a mapping between SOC models and the KPZ equation similar to that of Paczuski and Boettcher [22]. With this mapping, they have been able to obtain SOC from the KPZ equation with the proper kind of noise [21].

Moreover, roughening processes have also been found in the experimental SOC systems discussed above. The profile of a 1D rice pile is a rough interface [23], as is the front of magnetic flux penetrating a thin film superconducting sample [24]. However, the universal scaling relations derived by Paczuski *et al.* [14] have not yet been tested experimentally. But the fact that both roughening phenomena and avalanche dynamics can be observed in the same experimental system, such as a 3D rice pile, means that the universal connections between SOC and surface roughening can be tested experimentally.

Here, we present a two-dimensional (2D) system, the surface of a 3D pile of rice, showing both roughening behavior and avalanche dynamics. The avalanche dynamics is studied in terms of the avalanche size distribution for different sizes of the field of view, L. This allows the observation of finite size scaling and the determination of the critical exponents D, describing the dependence of the cutoff scale on L, and τ that is the exponent of the avalanche size distribution. The roughening behavior is studied via the power spectrum of the surface [25], in both space and time, resulting in a determination of the roughness and growth exponents, respectively [26]. The connection between these two phenomena is shown from the derivation of scaling relations between the different exponents, where we obtain an excellent agreement using the experimentally determined values.

The experimental setup for the growth of the rice pile, as well as the reconstruction method used to determine the

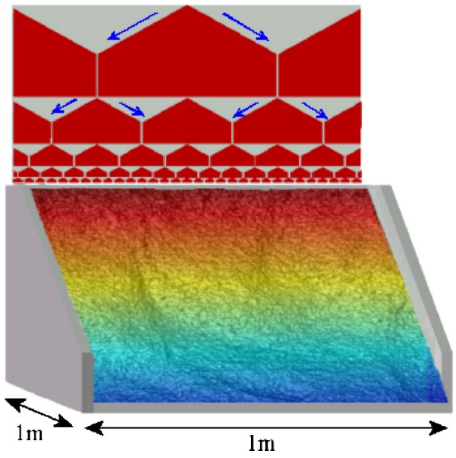

FIG. 1. A schematic image of the setup. The distribution board can be seen on top, where rice is dropped from a single point and subsequently divided into even compartments. Within the wooden box bounding the rice pile, a reconstruction of its surface is shown, as it is used in further analysis.

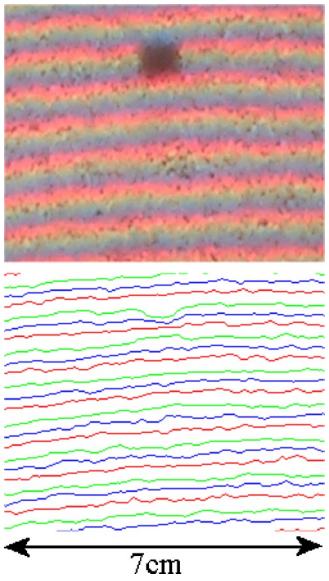

FIG. 2. A raw image of the rice pile with the identified lines. From the distortions of the lines, the surface geometry is obtained. The dark spot in the image indicates a reference point.

structure of the pile and the size of the avalanches, is discussed in Sec. II. The avalanche size distributions and their finite size scaling are presented in Sec. III A, together with the determination of the critical exponents. In Sec. III B, the surface roughness is analyzed and the necessary techniques are briefly introduced. Also, in this section, the scaling relations between the roughness exponents and the critical exponents are introduced. These results are also put into a wider context and compared with the results obtained from KPZ roughening systems [27].

II. EXPERIMENTAL DETAILS

The experiments were carried out on long grained rice with dimensions of typically $\sim 2\times 2\times 7$ mm^3, similar to rice *A* of Ref. [12]. The pile was grown from a uniform line source that is 1 m wide. This uniform distribution was achieved via a custom built mechanical distributor based on a nail board producing a binary distribution [28]. The actual setup consists of a board with an arrangement of triangles, as shown in Fig. 1. This means that the possible pathways of the rice are continuously split at each level, such that at the bottom we end up with a row of 64 uniformly distributed compartments. The uniformity of the distribution was measured to be of the order of 5%.

At the bottom of the distributor, the grains are slowed down by a sheet of plastic before they hit the top of the pile. The rice is fed to the top of the distribution board, from a point source, which drops rice at an average rate of ~ 5 g/s. This corresponds to 1500 grains per image, which means that over the length of the line the number of grains dropped per place ranges from one to two. This rate is uniform over the time scale between two images.

Once a rice pile is grown, we measure the further evolution of the surface coordinates using a specially developed real-time technique based on the projection of a set of lines. In order to increase the spatial resolution in the direction of growth, we use a set of lines in the base colors (red, green, and blue), which can be easily separated digitally for the analysis. The lines are projected at a right angle to the average surface of the pile and observed at 45° to both the direction of projection as well as the surface. This is illustrated in Fig. 2, where a raw image is shown together with the lines extracted from it. From the distortions of the lines observed in this way, the coordinates in the 3D space of the pile surface can be calculated by a simple geometry [28]. With this reconstruction technique, the 3D coordinates of the whole field of view can be determined with an accuracy of 2–3 mm, as we have checked on a number of test surfaces. Using both structured and smooth surfaces, the resolution and accuracy were determined independently. Since the resolution is roughly matched with the size of the grains, the method is well suited for the present purpose.

In a single experimental run, the growth is studied for a period of ~ 4 h, with a picture taken every 30 s. Thus, an experiment consists of ~ 480 images. The pictures are taken with a high resolution digital camera, having a resolution of 2048×1536 pixels. For every time step, the surface structure is reconstructed, which gives information about the roughening process, as well as the avalanche dynamics.

The size and shape of the avalanches can be determined from the height difference of the surface between two consecutive images. The overall growth of the pile is subtracted from this difference, however, this correction is negligible and does not influence the results. This is shown in Fig. 3, where the height difference $\Delta h(x,y)$ is shown for a medium sized avalanche. This allows one to study the internal avalanches instead of just the off-edge ones, which has proven to be important in previous studies (for instance, on superconducting vortex avalanches [11] and 1D piles of rice [12]). In order to obtain the size of such an avalanche, $|\Delta h|$ is integrated over the area, which yields the displaced volume ΔV, corresponding to the size of the avalanche in mm^3. In order to use natural units, we will in the following measure

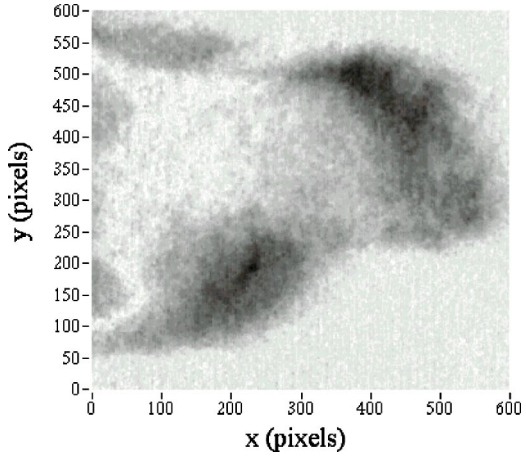

FIG. 3. A snapshot of an avalanche, given by the height difference of two subsequent images. In the picture, the height is given by the gray scale with white corresponding to $\Delta h=0$ and black to $\Delta h=15$ mm. Integrating the height difference $\Delta h(x,y)$ over the area gives the size of the avalanche in terms of volume, or in terms of the number of moved grains from the volume occupied by a grain $V_{grain}=35$ mm^3.

the size of the avalanche in terms of the number of toppled grains, which is $s=\Delta V/V_{grain}$, where $V_{grain}\simeq 35$ mm^3 is the volume of a single grain of rice.

The data discussed in this paper were obtained in three separate experiments with a total of 1330 images.

III. RESULTS

In this section, the experimental results are presented. We first show that there is finite size scaling in the avalanche statistics, which indicates the appearance of a critical state in the system. Second, we characterize the surface roughness of the rice pile in 2D, both in space and time. The two characteristic exponents, α for the spatial behavior and z for the dynamics [26], can also be obtained from scaling relations of the critical exponents of the avalanche statistics and are found to be in excellent agreement with those determined from a standard power-spectrum analysis.

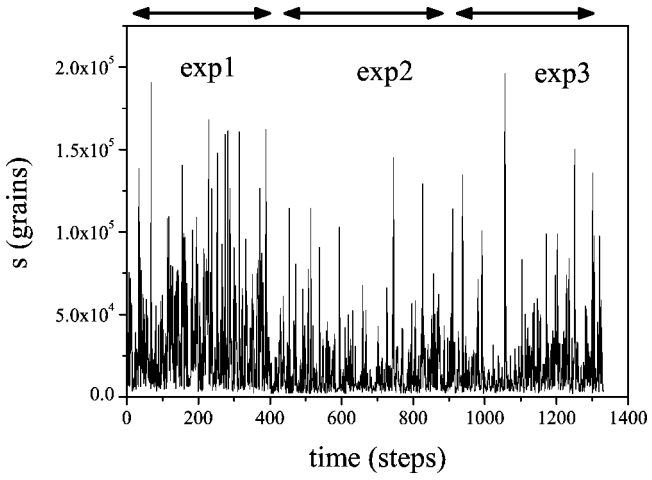

FIG. 4. The time evolution of the integrated height difference for the three experimental runs studied. As can be seen, times of relative rest are punctuated by large avalanches, which appear intermittently. When studying the distribution of avalanche sizes (see Fig. 5), it is found that there is no intrinsic size to the avalanches, but that they are distributed according to a power law. The different experimental runs are indicated by arrows.

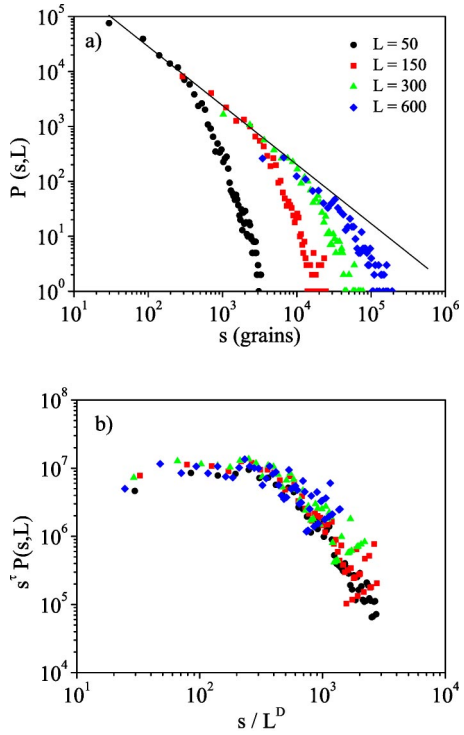

FIG. 5. (a) The unscaled size distribution functions for the avalanches from different subsets of the experiments corresponding to sizes of $L=50$, 150, 300, and 600 mm. Given the asymptotic dependence of all them together, there is power-law behavior over at least three decades, with an exponent of $\tau=1.20(5)$. (b) The same data scaled to produce a curve collapse. The sizes of the avalanches are scaled with L^{-D} and the probabilities are scaled with s^{τ}. The values used to obtain the best curve collapse are $\tau=1.21(2)$ and $D=1.99(2)$.

A. Avalanche dynamics

The time dependence of the displaced volume ΔV in each time step is shown in Fig. 4 for all the three experiments discussed here. In this figure, data are shown for avalanche sizes integrated over the total field of view of 600 $\times 600$ mm^2.

A histogram of these data, giving the avalanche size distribution, is shown by the diamonds in Fig. 5(a). In this figure, size distributions of subsets of the data, corresponding to smaller fields of view ($L=50$, 150, and 300 mm), are also shown. Due to experimental resolution, the smallest avalanches measured for each subset depend on the size of that subset. The range of sizes from 50×50 mm^2 to 600 $\times 600$ mm^2 spans more than a decade and all data taken together show a power-law scaling of the size distribution over three decades, with an exponent of $\tau=1.20(5)$.

These data can, however, be scaled to fall onto a single curve, as shown in Fig 5(b). Here, the avalanche sizes are

scaled with L^{-D} and the probabilities are scaled with s^{τ}. The good curve collapse visible in Fig 5(b) indicates the presence of finite size scaling in the data, one of the hallmarks of critical behavior in a system and thus an evidence of the appearance of SOC in the 3D rice pile. Due to the finite size scaling found from the curve collapse, the avalanche size distribution as a function of system size can be written as a function of one parameter only:

$$P(s,L)=s^{-\tau}f\left(\frac{s}{L^{D}}\right), \tag{1}$$

where $f(x)$ is constant up to a cutoff scale,

$$s_{co}\propto L^{D}. \tag{2}$$

The exponents τ and D used to obtain the curve collapse in Fig. 5(b) were $\tau=1.21(2)$ and $D=1.99(2)$. We note here that in the usual finite size scaling, separate experiments are used instead of subsets. However, as we have tested on simulations of a 2D version of the Oslo model [29], the finite size scaling using subsets yields the same exponents, but is much more easily implemented experimentally. As an additional test, the avalanche dimension can be determined directly using a box-counting method in 3D. This yields $D=2.05(10)$, consistent with the result from finite size scaling.

B. Surface roughening

The roughness of a surface can be characterized in different ways. Most commonly, this is done via the width of the interface as given by its standard deviation [26]. For a 2D surface, this is given by

$$w^2(L)=\frac{1}{L^2}\sum_{i,j=1}^{L}[h(i,j)-\langle h\rangle]^2, \tag{3}$$

where $\langle h\rangle$ is the average profile of the surface height. When the roughness of the surface has reached saturation, its value w_{sat} will scale with the system size as a power law, $w_{sat}\propto L^{\alpha}$, where α is the roughness exponent.

A similar type of analysis can be achieved via the power spectrum of the surface. Here, one has the advantage that better statistics can be obtained, since the whole surface can be used at once [25]. We determined the power spectrum from a radial average of the 2D Fourier transform of the surface,

$$S(k)=|\hat{h}(k_x,k_y)|^2, \tag{4}$$

where $k=(k_x+k_y)^{1/2}$. The Fourier transforms where performed via a fast Fourier transform algorithm, which is why a data subset corresponding to a power of two (512×512) was used. From the power spectrum we then determine the distribution function $\sigma(k)$,

$$\sigma^2(k)=\int_0^k S(\kappa)\kappa d\kappa, \tag{5}$$

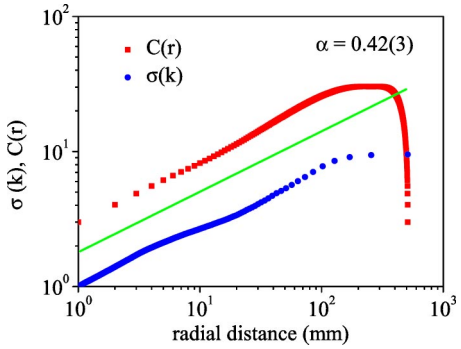

FIG. 6. Determination of the roughness exponent from a power-spectrum analysis as well as from the correlation function $C(x)$ (squares). After subtracting the average slope of the pile, its 2D power spectrum is calculated. After taking a radial average, it is integrated over k space in order to give the distribution function σ, which follows a power-law dependence $\sigma\propto k^{-\alpha}$, with a roughness exponent $\alpha=0.42(3)$. Similarly, the correlation function $C(x)\propto x^{\alpha}$ (squares) is calculated from the pile surface, resulting in the same exponent as that determined from the distribution function.

from which it can be shown [25] that $\sigma(2\pi/k)=w(\ell)$, where $\ell=2\pi/k$ is the length scale over which the width is calculated. The roughness exponent α can therefore be reliably obtained from the determination of $\sigma(k)$. An alternative way of obtaining the roughness exponent is via the two-point correlation function [26]

$$C(\vec{x},t)=(\langle[h(\vec{\xi},\tau)-h(\vec{x}+\vec{\xi},t+\tau)]^2\rangle_{\vec{\xi},\tau})^{1/2}, \tag{6}$$

the radial average of which obeys the same scaling behavior as the distribution function [26].

In Fig. 6, the correlation and distribution functions for the rice-pile surface are shown, averaged over all time steps of all experiments (1330 images). The part of the surface studied consists of 512×512 mm in the center of the surface laterally (along the horizontal direction) and starting from a height of 200 mm. As can be seen from the double logarithmic plot, there is power-law scaling with an exponent $\alpha=0.42(3)$.

The scaling behavior of the interface width can, however, also be determined from the cutoff size of the avalanches in a system with size L. The size of such an avalanche will be proportional to the maximal height difference, given by the saturation width w_{sat}, times the maximal area of the avalanche. As can be seen from Fig. 3, the avalanche shape is a fractal, which means that $s_{co}\propto w_{sat}L^{d_B}$, where d_B is the fractal dimension of the cluster of displaced grains. Equating this expression with Eq. (2), one obtains $w_{sat}\propto L^{D-d_B}$, which implies the scaling relation

$$\alpha=D-d_B. \tag{7}$$

Such a scaling relation between the roughness exponent and the exponents characterizing the avalanches was also derived by Paczuski *et al.* [14] from different arguments.

In order to determine d_B in an accurate manner, we studied avalanches more than two standard deviations larger than the average size. This corresponds to a subset of $\sim$100 im-

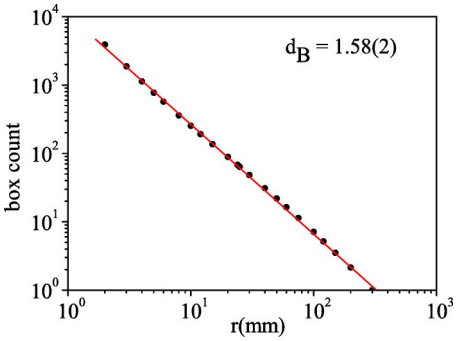

FIG. 7. Determination of the fractal dimension of the avalanches. Over all experiments, avalanches with a size two standard deviations larger than the average were studied. The contours are derived from a thresholding at the value of the mean height difference for each image. The fractal dimension is subsequently determined from a simple box-counting method.

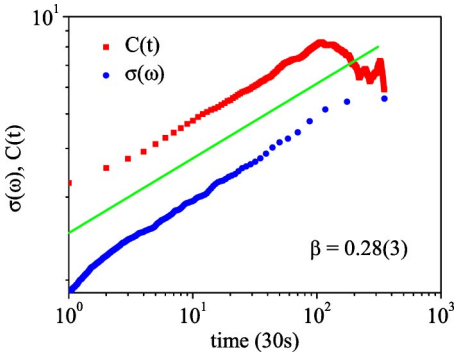

FIG. 8. Determination of the growth exponent from a power-spectrum analysis. Here, the distribution function σ has been determined from the time dependence of the height of each pixel. The data show a power-law dependence $\sigma \propto \omega^{-\beta}$, with a growth exponent $\beta = 0.28(3)$. The same result is obtained via the correlation function, indicated by open symbols. From the growth and roughness exponents, the dynamic exponent $z = \alpha/\beta = 1.5(1)$ can be determined.

ages from all experiments. After thresholding the height difference fields, $\Delta h(x,y)$, at their mean value, we applied a simple box-counting method [30] to the resulting clusters. This is shown in Fig. 7, where the number of active pixels in a box of given size is shown as a function of the box size. The result is a power law with an exponent of $-1.58(2)$, indicating a fractal dimension of $d_B = 1.58(2)$. Inserting this value into scaling relation (7), the roughness exponent is found to be $\alpha = 0.41(3)$, in excellent agreement with that determined from the roughness analysis.

The dynamics of the roughening process is likewise analyzed via the distribution function. In contrast to the roughness analysis above, we now determine the distribution function for the time dependence $h_{i,j}(t) - \langle h_{i,j} \rangle_t$ for each pixel, where $\langle \cdots \rangle_t$ denotes the average over the duration of the experiment. Again, the distribution function given by

$$\sigma^2(\omega) = \int |\hat{h}(\omega)|^2 d\omega \tag{8}$$

is equal to the momentary width $\sigma(2\pi/\omega) = w(t)$. Thus, the growth exponent β, describing the scaling of the width with time, can be determined from the distribution function. Again, the correlation function shows the same scaling behavior in time, allowing a separate determination of β. Both results are shown in Fig. 8, where it can be seen that there is a good power-law scaling of the distribution function, as well as the correlation function, over two decades with an exponent of $\beta = 0.28(3)$. Another way of describing the dynamics of an interface is via the dynamic exponent z, which describes the scaling of the saturation time with the system size,

$$t_\times \propto L^z. \tag{9}$$

It can be easily obtained [26] from the roughness and growth exponents via

$$z = \frac{\alpha}{\beta}. \tag{10}$$

From the values determined above, we thus obtain $z = 1.5(1)$.

The dynamic exponent z can also be derived from a scaling relation using the critical exponents of the avalanche dynamics. The saturation time $t_\times$ will be roughly given by the time it takes for an avalanche of the cutoff size s_{co} to appear. Since material is added to the system at a constant rate, the number of grains added until a cutoff avalanche occurs is proportional to the crossover time $t_\times$. On the other hand, the material added not only results in an avalanche of size s_{co}, but will also be lost by smaller avalanches, such that the total material necessary to obtain an avalanche of size s_{co} can be estimated from

$$\int_0^{s_{co}} sP(s)ds \propto s_{co}^{2-\tau}. \tag{11}$$

From Eq. (2), we obtain for the crossover time $t_\times \propto L^{D(2-\tau)}$. With Eq. (9), this immediately leads to the scaling relation

$$z = D(2-\tau), \tag{12}$$

which was also derived by Paczuski *et al.* [14] from more general arguments. Using the values for D and τ determined above from the curve collapse of the avalanche size distributions, we obtain $z = 1.56(8)$, which is again in very good agreement with the result of the power-spectrum analysis, $z = 1.5(1)$. Note also that the exponents α and z fulfill the KPZ scaling relation [19] $\alpha + z = 2$, which is valid independent of the dimension of the system and depends only on the fact that the growth is driven by height gradients. Furthermore, the roughness exponent $\alpha = 0.42(3)$ is in good agreement with a numerical determination of the behavior of the 2D KPZ equation [27]. The connection between roughening and SOC will be discussed in more detail below.

IV. CONCLUSIONS

In conclusion, we have presented results of both the avalanche and the roughening behavior of an experimental SOC system. In addition, we presented simple arguments for universal scaling relations, derived by Paczuski *et al.* [14] on general grounds, connecting the avalanche and the roughening behavior. We obtain a *quantitative* agreement of the experimental exponents characterizing the roughness and those describing the avalanche statistics. This means that the roughening of the surface of the pile is governed by its underlying avalanche dynamics, which was already conjectured from models of interface depinning. Earlier experimental studies [12,23] have considered the avalanche dynamics and the roughening behavior of the 1D version of the present system, where finite size scaling was also found [12]. The above scaling relations, showing quantitatively the connection between the two phenomena, were not previously tested.

The fact that KPZ dynamics is observed in an SOC system, as indicated by the fact that the roughness and dynamic exponents obtained here fulfill the KPZ scaling relation, is surprising. This is mostly because in SOC systems, the critical state is self-organized, whereas in KPZ systems, the roughening is put into the dynamics by obeying the proper symmetries. However, it has been argued by Alava and coworkers [21] that there is a mapping of SOC models, which naturally lead to the necessary symmetries. In this context, it should also be noted that experiments on KPZ systems such as burning paper have also observed avalanches in the advance of fronts [20].

ACKNOWLEDGMENTS

This work was supported by FOM (Stichting voor Fundamenteel Onderzoek der Materie), which is financially supported by NWO (Nederlandse Organisatie voor Wetenschappelijk Onderzoek).

[1] P. Bak, C. Tang, and K. Wiesenfeld, Phys. Rev. Lett. **59**, 381 (1987); Phys. Rev. A **38**, 364 (1988).
[2] O. Peters, C. Hertlein, and K. Christensen, Phys. Rev. Lett. **88**, 018701 (2002); O. Peters and K. Christensen, Phys. Rev. E **66**, 036120 (2002).
[3] P. Bak, K. Christensen, L. Danon, and T. Scanlon, Phys. Rev. Lett. **88**, 178501 (2002); A. Sornette and D. Sornette, Europhys. Lett. **9**, 197 (1989); J.M. Carlson, J.S. Langer, and B.E. Shaw, Rev. Mod. Phys. **66**, 657 (1994).
[4] J.A. Scheinmann and M. Woodford, Am. J. Agric. Econom. **84**, 417 (1994); P. Bak, K. Chen, J.A. Scheinmann, and M. Woodford, Ricerche Economiche **47**, 3 (1993).
[5] J. Bascompte and R.V. Solé, Trends Ecol. Evol. **10**, 361 (1995); H. Flyvbjerg, P. Bak, and K. Sneppen, Phys. Rev. Lett. **71**, 4087 (1993); S.A. Kaufmann and S.J. Johnsen, J. Theor. Biol. **149**, 467 (1991).
[6] D. Stassinopoulos and P. Bak, Phys. Rev. E **51**, 5033 (1995).
[7] H.M. Jaeger, S.R. Nagel, and R.P. Behringer, Rev. Mod. Phys. **68**, 1259 (1996); S.R. Nagel, *ibid.* **64**, 321 (1992), and references therein.
[8] S. Field, J. Witt, and F. Nori, Phys. Rev. Lett. **74**, 1206 (1995); C.M. Aegerter, Phys. Rev. E **58**, 1438 (1998).
[9] R.J. Zieve, T.F. Rosenbaum, H.M. Jaeger, G.T. Seidler, G.W. Crabtree, and U. Welp, Phys. Rev. B **53**, 11 849 (1996); E.R. Nowak, O.W. Taylor, L. Liu, H.M. Jaeger, and T.I. Selinder, *ibid.* **55**, 11 702 (1997).
[10] J. Feder, *Fractals* (Plenum, New York, 1989).
[11] K. Behnia, C. Capan, D. Mailly, and B. Etienne, Phys. Rev. B **61**, R3815 (2000); J. Magn. Magn. Mater. **226**, 370 (2001).
[12] V. Frette, K. Christensen, A. Malthe-Sørenssen, J. Feder, T. Jøssang, and P. Meakin, Nature (London) **379**, 49 (1996).
[13] E. Altshuler, O. Ramos, C. Martinez, L.E. Flores, and C. Noda, Phys. Rev. Lett. **86**, 5490 (2001).
[14] M. Paczuski, S. Maslov, and P. Bak, Phys. Rev. E **53**, 414 (1996).
[15] M.A. Rubio, C.A. Edwards, A. Dougherty, and J.P. Gollub, Phys. Rev. Lett. **63**, 1685 (1989); V.K. Horváth, F. Family, and T. Vicsek, J. Phys. A **24**, L25 (1991); S. He, G.L.M.K.S. Kahanda, and P.-Z. Wong, Phys. Rev. Lett. **69**, 3731 (1992).
[16] E. Ben-Jacob, O. Shochet, A. Tenenbaum, I. Cohen, A. Czirók, and T. Vicsek, Nature (London) **368**, 46 (1994); S. Matsuura and S. Miyazima, Fractals **1**, 336 (1993); T. Vicsek, M. Cserzö, and V.K. Horváth, Physica A **167**, 315 (1990).
[17] J. Maunuksela, M. Myllys, O.P. Kähkönen, J. Timonen, N. Provatas, M.J. Alava, and T. Ala-Nissila, Phys. Rev. Lett. **79**, 1515 (1997).
[18] J. Kertész, V.K. Horváth, and F. Weber, Fractals **1**, 67 (1993).
[19] M. Kardar, G. Parisi, and Y.-C. Zhang, Phys. Rev. Lett. **56**, 889 (1986).
[20] A. Myllys, J. Maunuksela, A. Alava, T. Ala-Nissila, J. Merikoski, and J. Timonen, Phys. Rev. E **64**, 036101 (2001); J. Timonen (private communication).
[21] M. Alava and K.B. Lauritsen, Europhys. Lett. **53**, 569 (2001); G. Szabo, M. Alava, and J. Kertesz, *ibid.* **57**, 665 (2002); M. Alava, J. Phys. C **14**, 2353 (2002).
[22] M. Paczuski and S. Boettcher, Phys. Rev. Lett. **77**, 111 (1996).
[23] A. Malthe-Sørenssen, J. Feder, K. Christensen, V. Frette, and T. Jøssang, Phys. Rev. Lett. **83**, 764 (1999).
[24] R. Surdeanu, R.J. Wijngaarden, E. Visser, J.M. Huijbregtse, J.H. Rector, B. Dam, and R. Griessen, Phys. Rev. Lett. **83**, 2054 (1999).
[25] J. Schmittbuhl, J.-P. Vilotte, and S. Roux, Phys. Rev. E **51**, 131 (1995); M. Siegert, *ibid.* **53**, 3209 (1996); J.M. Lopez, M.A. Rodriguez, and R. Cuerno, *ibid.* **56**, 3993 (1997).
[26] A.L. Barabasi and H.E. Stanley, *Fractal Concepts in Surface Growth* (Cambridge University Press, Cambridge, 1995).
[27] J.G. Amar and F. Family, Phys. Rev. A **41**, 3399 (1990).
[28] R. Günther, Masters thesis, Vrije Universiteit, 2002 (unpublished).
[29] C.M. Aegerter, Physica A **319**, 1 (2003).
[30] B.B. Mandelbrot, *The Fractal Geometry of Nature* (Freeman, New York, 1983).